# IMPROVED NIST AIRSPEED CALIBRATION FACILITY.

**Iosif I. Shinder**
NIST
100 Bureau Dr.
Gaithersburg, MD
20899-8361
301-975-5943
ishinder@nist.gov

**James R. Hall**
NIST
100 Bureau Dr.
Gaithersburg, MD
20899-8361
301-975-5947
mikehall@nist.gov

**Michael R. Moldover**
NIST
100 Bureau Dr.
Gaithersburg, MD
20899-8360
301-975-5943
MMoldover@nist.gov

*Abstract-The National Institute of Standards and Technology (NIST) uses a laser Doppler anemometer (LDA) as a working standard for airspeed calibrations in the range 0.2 m/s to 75 m/s (0.45 to 168 miles/hour). We report improved procedures for calibrating the LDA that reduced its uncertainty from 0.26% to 0.10% at airspeeds above 1 m/s. (Uncertainties are stated with the coverage factor k=2 which corresponds to a 95 % confidence level.) The calibration uses a rotating disk with known dimensions at several known rotation frequencies, thereby tracing the LDA to the primary standards of length and time. We also improved the LDA signal-to-noise ratio in NIST's wind tunnel, particularly at higher air speeds, by replacing a water seeding system with an oil seeding system. New software automates the airspeed setting, oil-seeding rate, data-collection time, and instrument averaging time.*

## INTRODUCTION

The National Institute of Science and Technology (NIST) calibrates a wide variety of anemometers including Pitot static tubes, hot wire based instruments, various mechanical anemometers, and acoustic anemometers. The NIST airspeed calibration service helps airspeed instrument manufacturers and users as well as research institutions by to enabling these customers to trace their airspeed measurements to the US National Airspeed Standard maintained by NIST. NIST's service operates in the airspeed range 0.2 m/s to 75 m/s (0.45 to 168 miles/hour) and has an expanded relative uncertainty $U_r(V) = 0.001 + 0.02/V$, where $V$ is the airspeed expressed in meters/second. (Uncertainties are stated with the coverage factor $k$=2 which corresponds to a 95 % confidence level). Recently, NIST modernized its airspeed service by improving the procedures for calibrating the working standard (laser Doppler anemometer "LDA"), by replacing a water seeding system with an oil seeding system, automating data collection, and upgrading data acquisition software.

## WIND TUNNEL

NIST's Dual Test Section Wind Tunnel is a toroid-shaped, closed-loop structure lying in a horizontal plane (Fig. 1). The wind tunnel has two interchangeable test sections that are used to span the range of airspeeds from 0.2 to 75 m/s. Both test sections are 12 m long; however, their cross-sections differ. The low-speed test section is used for calibrations ranging from 0.2 m/s to 45 m/s and it is 2.1 m high and 1.5 m wide. The high-speed test section is used for airspeed calibrations up to 75 m/s. Its height gradually decreases from 2.1 m to 1.2 m along the flow direction, forming a venturi-like duct. Both test sections provide longitudinal free-stream turbulence levels of 0.07 % over most of the airspeed range and a transverse velocity gradient of less than 1% within a working area of 90% of the test section areas. More detailed information about NIST Airspeed Calibration Facility can found in [1, 2]. Here, we describe recent improvements to NIST's airspeed calibration services including a new procedure for calibrating the laser Doppler anemometer (LDA) with a rotating disk, a new seeding system, and improved software.
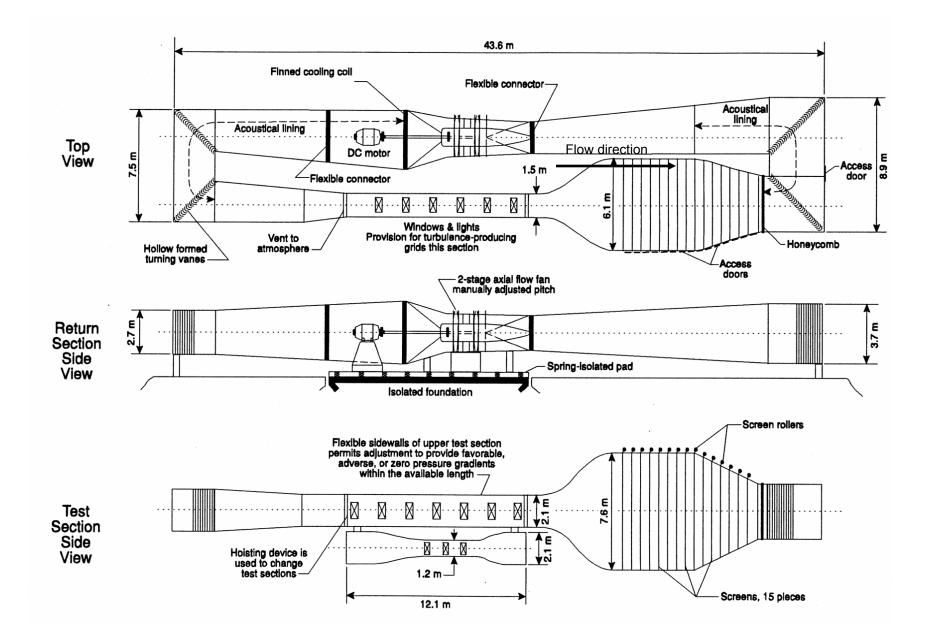
Figure 1. NIST dual section wind tunnel

# SEEDING

A high-quality seeding system is essential for fast, accurate LDA measurements. From 2004 until 2009, NIST used simple sprays to inject water droplets into the wind tunnel. (See Fig. 2.) As a seeding compound, water is safe because it is neither flammable nor toxic. However, the water seeding system had significant drawbacks:

   1. The droplets produced by the sprays were comparatively large. They had a mean diameter of approximately 50 micrometers and a wide size distribution ranging from 1 micrometer to 1000 micrometers.

   2. The evaporation rate of the droplets depended on the temperature and humidity of the air in the wind tunnel. On dry days and at high airspeeds, the
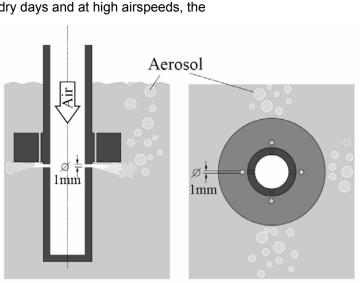


Figure 2. Water sprays.

temperature might rise 40 ºC and the relative humidity would drop to 10 %. Then, the droplets evaporated quickly and LDA signal-to-noise ratio decreased. To compensate, we increased seeding rate. However, this had negative consequences; the larger-diameter droplets were deposited on the tunnel's walls and flow-conditioning screens causing them to deteriorate. The tap water had dissolved solids that deposited on the flow-conditioning screens and clogged their apertures.

   3. The wide droplet size distribution led to non-uniform seeding.

   4. We were concerned that mechanical anemometers, such



Figure 3. Individual Laskin nozzle

as propellers, might be affected by the momentum transferred from the larger droplets.

In order to improve the seeding system, we tested several smog machines, fog generators, and oil atomizers. Ultimately, we chose to generate oil droplets using the atomizer PivPart45-M[*] series, manufactured by the PIVTEC company, Germany. This atomizer generates droplets using the Laskin method. (See Fig. 3.) Air is supplied to each Laskin nozzle at a gauge pressure of 50 kPa to 100 kPa. The air flow generates bubbles within the liquid. These bubbles

---

[*] In order to describe materials and procedures adequately, it is occasionally necessary to identify commercial products by manufacturer's name or label. In no instance does such identification imply endorsement by the National Institute of Standards and Technology, nor does it imply that the particular product or equipment is necessarily the best available for the purpose.
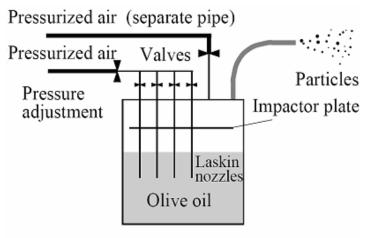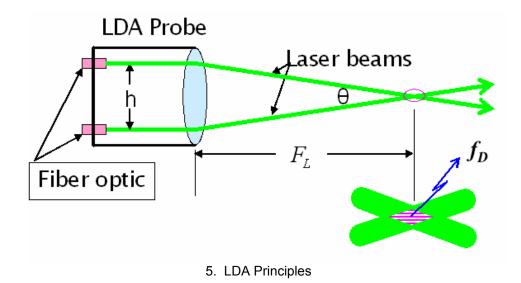
Figure 4. Droplet generator.

rise and then burst at the liquid-air surface. The bursting creates small droplets with a narrow size distribution. The droplets are swept by the air flow out of the generator into the wind tunnel. The generator (Fig. 4) is a closed cylindrical container with two air inlets and one aerosol outlet. One of the air inlets feeds four air-supply pipes leading to the Laskin nozzles immersed in the oil. The PivPart45-M series generator has 45 Laskin nozzles which can be used in series of triplets 3, 6, 9… and up to 45 nozzles. We tested non-toxic oils including vegetable oils, oleic acid, di-ethyl-hexyl-sebacate (DEHS), commercially-sold fog fluids, and water. All of the oils tested produced stable droplets with a mean diameter of about 1 micrometer. At air speeds below 10 m/s, the droplets persisted in the tunnel for hours after the atomizer was turned off. Using 27 out of 45 Laskin nozzles, we produced stable LDA data acquisition rates ranging from 100 Hz to 10000 Hz for entire airspeed range. During typical tests extending from 0.2 m/s to 75 m/s and lasting 4 hours, we used from 3 grams to 10 grams of oil. The literature reports [3] that a 0.3 micrometer diameter droplet evaporates in approximately 4 hours at room temperature. We measured the evaporation of oleic acid and DEHS. One gram of oil evaporates from a wetted piece of cloth with area of 10 cm$^2$ in approximately 30 minutes at airspeeds from 20 m/s to 75 m/s. Thus, the DEHS droplets will not accumulate on the surfaces of either the wind tunnel or of the instruments tested in the tunnel. We prefer to use DEHS instead of oleic acid because DEHS has no odor.

## LDA PRINCIPLES AND CALIBRATION

Differential Laser Doppler Anemometry is widely used to measure particle velocities. The anemometer has two converging laser beams that overlap to establish an interference pattern composed of nearly-parallel dark and bright fringes (Fig. 5). As a droplet passes through each bright fringe, it scatters light. Therefore, the scattered light blinks on and off at a frequency



5. LDA Principles

Table 1. Parameters of NIST's LDA system.

| | |
|---|---|
| Laser wavelength $\lambda$ | 514.5 nm |
| Laser beam separation $h$ | 73.7 mm |
| Focal length $F_L$ | 1200 mm |
| Beam intersection angle $\theta$ | 3.52 deg |
| Fringe spacing $d$ | 8.38 mm |
| Probe diameter $d_m$ | 0.35 mm |
| Probe length $l_m$ | 11.5 mm |

proportional to the droplet's velocity divided by the distance between the bright fringes. This method measures the component of the particle's velocity in the plane of the converging beams and in the plane perpendicular to the plane bisecting the two converging laser beams [4]. Table 1 lists the main parameters of NIST's LDA system. Details of the performance, calibration, and uncertainty of NIST's LDA analysis can be found in [1]. The airspeed is calculated with the equation: $V_{LDA} = d\,f_D$, where $f_D$ is Doppler frequency and $d$ is fringe spacing. The fringe spacing can be calculated from the angle between the intersecting beams $\theta$, the focal length of the lens $F_L$, and the laser wavelength $\lambda$ using the equation:

$$d = \lambda / \left[ 2\sin\left(\theta/2\right) \right] \quad .$$

Alternatively, the LDA system can be calibrated using well-defined velocities generated by a rotating disk. Reference [5] shows that both methods lead to the same result. At present, NIST calibrates its LDA system using a rotating disk with a diameter $D$ =136 mm (Fig. 6). A 12 µm diameter wire is mounted on the rim of a disk. The disk and the light-scattering wire rotate at a measured rotation frequency $f_{disk}$. The tangential speed of the wire $V_{disk}$ is:

$$V_{disk} = f_{disk} D / 2$$

The LDA is aligned so that the plane bisecting the intersecting light beams is parallel to and passes through the axis of the disk and the wire passes through the intersection volume as the disk rotates. In this way, the LDA measures the known speed $V_{disk}$ produced by the rotating disk. The calibration factor, $C_{LDA}$ is determined from the disk's speed and the speed indicated by the LDA using relation $C_{LDA} = V_{disk} / V_{LDA}$
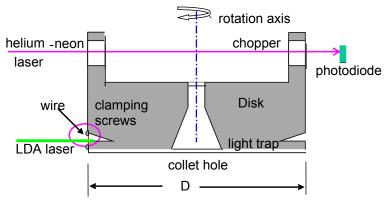


Figure 6. Rotating disk.

# ROTATING DISK ALIGNMENT

Recently, we improved our calibration procedure by paying more attention to aligning the laser beam relative to the rotating disk. As shown in 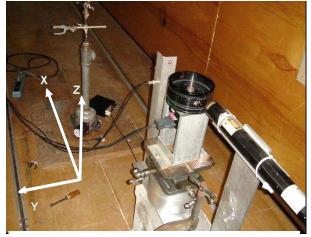Figure 7, the rotating disk is supported on a heavy, disk-shaped pedestal that is attached (with two-sided tape) to a frame that also supports a laser and photodiode detector that are used for alignment and for measuring the rotation frequency of the disk. The frame is attached to a heavy cinder block using a C-clamp (Fig. 7).



Figure 7. Rotating disk installation and coordinate system.

For alignment, the center of the rotating disk is first adjusted in the X-direction, *i.e.*, in the direction of the air flow. The rotating disk is removed from pedestal. The traversing mechanism below the rotating disk (red arrow) is adjusted until the two laser spots (green arrows) are symmetrical on the rotating disk's shaft (Fig. 8). Next, the disk is replaced on its pedestal and the Z-coordinate (height) is adjusted (Fig. 9). This step uses the software that the manufacturer supplied with the burst spectrum analyzer (BSA). The software controls a 2-D traverse system that adjusts the laser beams to the height of the center of the wire.

The last step, the Y-coordinate alignment, is more complicated. The Y-coordinate was adjusted by eye to within $\pm 1$ mm of the center of the intersecting laser beams of the LDA. Then we examined the spectrum generated by the BSA (See Fig. 10). Fine adjustments were made to the Y-coordinate until the burst spectrum was
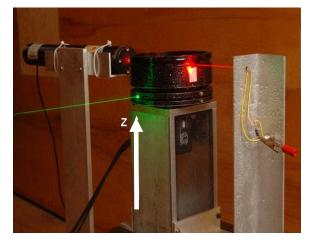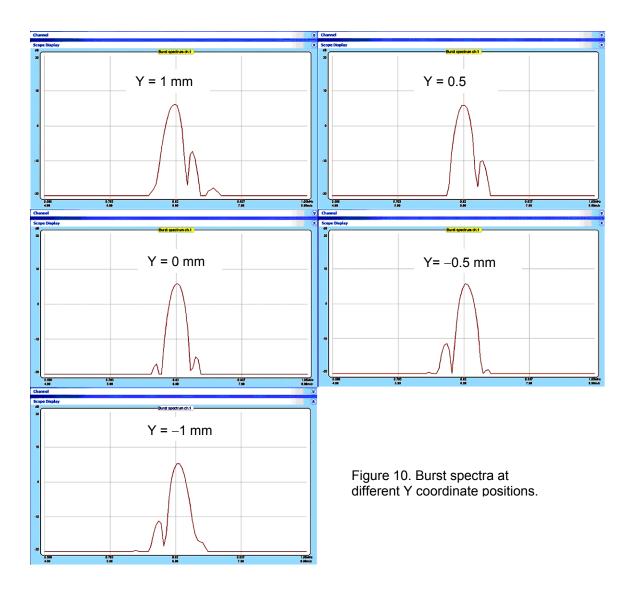


Figure 8. X-coordinate alignment.

symmetrical in the *Y*-coordinate. The precision of this adjustment was approximately $\pm 0.1$ mm. The position of the rotating disk was visually examined at the end of this procedure; no changes were visible.



Figure 9. Z-coordinate alignment

Figure 10. Burst spectra at different Y coordinate positions.

# ROTATING DISK CALIBRATION

Calibration is conducted in two steps. First, LDA is compared with the spinning disk while the wire is at the center of the intersecting laser beams. Second, the comparison is repeated as a function of the $Y$-coordinate. Once the laser sensing volume is aligned, measurements are taken at the same position for 16 different speeds in the range from 0.25 m/s to 40 m/s. Three measurements are made at each speed resulting in a total of 48 measurements. At each speed, at least 580 LDA points are acquired. This process is time-consuming at low speeds. For example, the data acquisition at 0.25 m/s takes about 17 minutes. A plot of true speed (rotating disk speed) vs. LDA measured speed is shown on Fig. 11. The data are fit by a straight line with the slope 1.00255±0.00007. The second part of calibration is to estimate uncertainty due to imperfect $Y$-coordinate alignment. Fig. 12 shows the dependence of the LDA measurements on $Y$ at three air speeds. The largest slope, $8 \times 10^{-3}$/mm, occurs at 40 m/s. Conservatively, we used this value for the uncertainty calculations at all air speeds. As mentioned above, the Y position of the beams can be found within ±0.1 mm which corresponds to the relative velocity uncertainty ±0.0008 $V_{disk}$. Assuming a rectangular distribution, the relative uncertainty of an air speed calibration due to the Y position is $0.0008/(3)^{1/2} \approx 5 \times 10^{-4}$. This value is much bigger than the uncertainty of the slope; therefore the uncertainty of the slope can be neglected when the total expanded uncertainty is calculated.
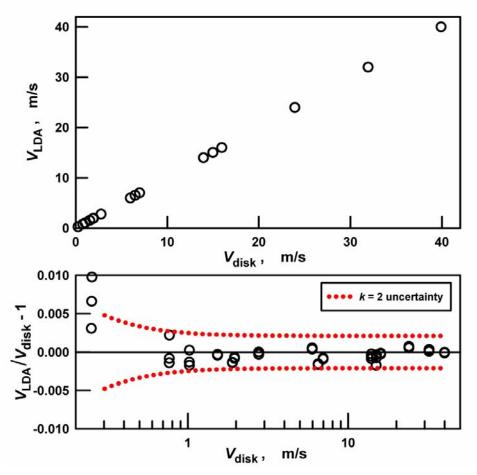


Fig. 11. Laser Doppler velocities compared to spinning disk velocities and uncertainties of linear fit.
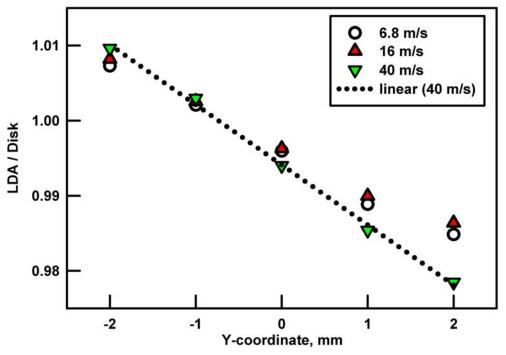
Figure 12. Calibration coefficient as a function of the Y-coordinate.

Currently the expanded ($k$=2) uncertainty of NIST's Airspeed Standard is
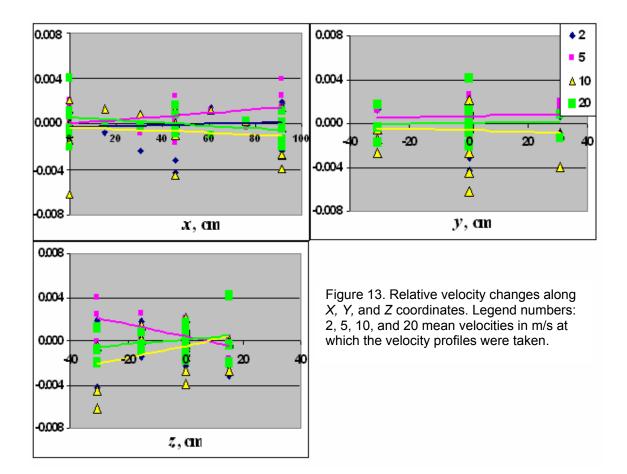
$$U = \sqrt{\left(0.0036\, m/s\right)^2 + \left(0.0064\, V_{LDA}\right)^2}$$

After we document the improvements described in this manuscript we expect the total uncertainty will be reduced by 20 % to 30%. We note that the uncertainty of the calibration coefficient is small and, in theory, it is independent of the air speed. However, LDA measurements at speeds below 1 m/s have a larger uncertainty. In our case, the time allowed for data-collection at low speeds is limiting; therefore, the uncertainty grows as $1/V_{LDA}$ and reaches 1 % to 2 % of $V_{LDA}$ at 0.2 m/s. (See Fig. 11).

## VELOCITY PROFILE UNCERTAINTY

In order to estimate the part of calibration uncertainties connected with the location of the instrument under test (IUT), we measured velocity profiles for different airspeeds. To measure the velocity profile we used our primary standard, LDA, as a reference and we used a Pitot tube as a survey device. The ratio of the Pitot tube calibration factor at different locations is a measure of a bias connected with the position of the IUT with respect to the primary standard. We found that the ratio of calibration factors (Fig. 13) at $x$, $y$, $z$ coordinate to the calibration factor at 0, 0, 0 coordinate location can be described by formula:

$$\frac{V_{xyz}}{V_{000}} = \left(1.0101 \pm 0.0004\right) + \left(-0.0138 \pm 0.0012\right)\left(\frac{m/s}{V_{000}}\right) + \frac{10^{-5}}{cm} \times \left[\left(8.7 \pm 0.6\right)x + \left(-1.3 \pm 1.3\right)y + \left(-4.7 \pm 1.5\right)z\right]$$

Figure 13. Relative velocity changes along *X, Y,* and *Z* coordinates. Legend numbers: 2, 5, 10, and 20 mean velocities in m/s at which the velocity profiles were taken.

The biggest bias connected with IUT location is along the x coordinate.  During typical calibrations, the IUT is located 10 to 15 cm downstream of the LDA sensing volume.  There, the bias approaches 0.1% and can be neglected.

## AIRSPEED MEASUREMENT AUTOMATION AND SOFTWARE.

NIST airspeed service uses LabView software to control data acquisition. The block diagram of data acquisition program is shown on Fig. 14. Blue rectangular boxes and arrows are recently added connections, virtual instruments and hardware.

Before this update, the operator had to turn a potentiometer by hand to set each airspeed. This manual airspeed control was replaced by a virtual instrument that controls the fan's power supply. Now, the operator can set air speeds manually or enter a table of airspeeds to be used during calibrations. LDA data acquisition was updated. Before this update, the LDA-data were acquired manually and were added to the IUT data table after the calibrations were completed.  The ActiveX control connects the LDA computer software so that the value of LDA measured airspeed is in the data output file. The main program monitors the data rate. When the data rate is too low the main program turns on the atomizer; if the date rate is higher than necessary it turns the atomizer off.
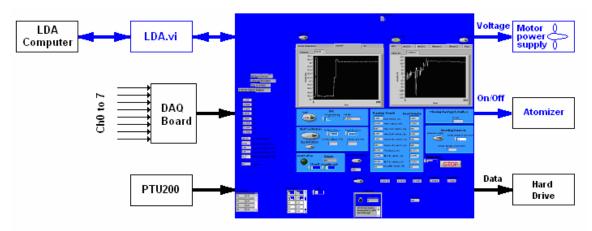
Figure 14. Block diagram of the data acquisition program.

## CONCLUSIONS

We have reported several significant upgrades to the NIST Airspeed Calibration facilities.  By improving the technique for calibrating our LDA Spinning Disk Calibrator, we have been able to decrease the uncertainty of the LDA standard to 0.1%. The wind tunnel software now operates both the wind tunnel and the data acquisition. Major improvements in data rate have been achieved by switching from water/air nozzles to Laskin nozzles and a volatile oil (DEHS). In the near future, we will re-evaluate the uncertainty budget for the entire Airspeed Calibration Facility. We also plan to add the ability to calibrate 3-dimensional probes by rotating, under computer control, the instrument under test relative to the direction of the air flow.

## REFERENCES.

[1] T.T. Yeh, M.J. Hall. *Airspeed Calibration Service.* NIST Special Publication SP 250-73.
[2] N.E. Mease, W.G. Cleveland, Jr., G.E. Mattingly, and J.M. Hall. *Airspeed Calibration at the National Institute of Science and Technology.* Proceedings of the 1992 Measurement Science Conference, Anaheim, California.
[3] Topaz GmbH. http://www.topas-gmbh.de/_DEHS_en.htm
[4] L.E. Drain. *The Laser Doppler Technique.* A Wiley-Interscience Publication, 1980.
[5] Vern E. Bean, J. Michael Hall. *New Primary Standard for Airspeed measurement at NIST*, Proceeding of 1999 NCSL Workshop and Symposium, p.413].